Chemical Physics Letters 866 (2025) 141965

Contents lists available at ScienceDirect

Chemical Physics Letters

journal homepage: www.elsevier.com/locate/cplett

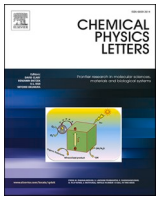

Temperature programmed desorption study of pre-irradiated TiO_2 anatase in the presence of ethanol. Effect of conduction band electrons on reaction selectivity

M.A. Nadeem [a], H. Idriss [b,*]

[a] Surface Science and Advanced Characterization, SABIC-CRD at KAUST, Thuwal 23955, Saudi Arabia
[b] Institute of Functional Interfaces (IFG), Karlsruhe Institute of Technology (KIT), 76344 Eggenstein-Leopoldshafen, Germany

ARTICLE INFO

Keywords:
TiO_2 Anatase
Ethanol-TPD
UV excitation
Infrared spectroscopy TiO_2
Conduction band electrons

ABSTRACT

The work addresses one of the fundamentals of photocatalytic reactions, the fate of conduction-band (CB) electrons of a photo-excited TiO_2-anatase. Some of these CB-electrons are self-trapped as large-polarons. We have studied by Infrared-spectroscopy these polarons upon UV-excitation in the presence and absence of O_2. Moreover, the effect of CB-electrons on chemical reactions was investigated by temperature-programmed-desorption. Over the non-irradiated TiO_2, the dehydration and oxidation products dominated, while over that prior UV-irradiated in the presence of ethanol the dehydrogenation product increased and the oxidation pathway was partly suppressed. These changes are attributed to CB-electrons that made the near-surface more metallic.

1. Introduction

Changes in products selectivity in catalytic reactions are sensitive to the nature of the catalyst as well as to reaction conditions. In that regards, decades of work have been devoted to understand the effect of the nature of catalytic sites on reaction products. To give a few examples, CO molecular versus dissociative adsorption/reaction on different metals [1], which is relevant to Fisher Tropsch synthesis [2] from syngas, C3 and C4 oxidation [3] to aldehydes and carboxylic acids versus dehydrogenation to olefins [4] over mixed metal oxides, and reaction pathways of primary and secondary alcohols over metal oxides [5,6].

In general, reducible metal oxides orient more towards dehydrogenation to aldehydes/ketones of alcohols while non reducible metal oxides orient towards dehydration to olefins [7]. While this is a simplistic picture, because it does not consider surface structure effect, among many other factors, it does help as a guide. In that scheme TiO_2 is considered amphoteric in a sense that both compounds are formed with a bias towards the dehydration reaction. Focusing on ethanol one can divide its reaction into three main ones.

The first is its dissociative adsorption leading to ethoxides and surface hydroxyls. This reaction is sensitive to TiO_2 phase [8] and different surface orientations [9], among other factors.

The second is the reaction of ethoxides to ethylene and acetaldehyde [10], this usually occurs at temperatures above 500 K and depends on the presence or absence of surface oxygen defects [11] in addition.

The third is the further reaction mostly of acetaldehyde, since ethylene because of its relative inertness on TiO_2 and weak adsorption energy does not further react once formed. Acetaldehyde can undergo many additional reactions such as aldol condensation to C_4 unsaturated aldehyde (crotonaldehyde) [12], oxidation to acetates [13] which decompose to methane and CO_2 at higher temperatures [14], in which CH_4 may also reform [15] to CO and H_2 with water formed during the dehydration reaction.

TiO_2 is also an n-type semiconductor that is found to be active for the photocatalytic oxidation of hydrocarbons [16,17] in the presence of O_2. It is also active for the photo-reforming of alcohols [18,19] to H_2 and CO_2. The photo-reforming reaction requires a metal in addition in order to trap conduction band electrons [20] Schottky barrier) as well as to recombine hydrogen atoms to molecular hydrogen [21]. In the absence of a metal far less formation of H_2 occurs [22,23]. In this process ethanol (or more precisely an ethoxide species [24,25]) injects electrons into the valence band to trap holes allowing conduction band electrons to reduce hydrogen ions of surface hydroxyls to atomic hydrogen. In the absence of a metal, part of these conduction band electrons either recombine with un-trapped holes, but another is self-trapped as polarons. These polarons are Ti^{3+} (Ti^{4+} that was reduced under UV light) in which this

* Corresponding author.
E-mail addresses: h.idriss@ucl.ac.uk, Hicham.idriss@kit.edu (H. Idriss).

https://doi.org/10.1016/j.cplett.2025.141965
Received 15 December 2024; Received in revised form 1 February 2025; Accepted 11 February 2025
Available online 13 February 2025

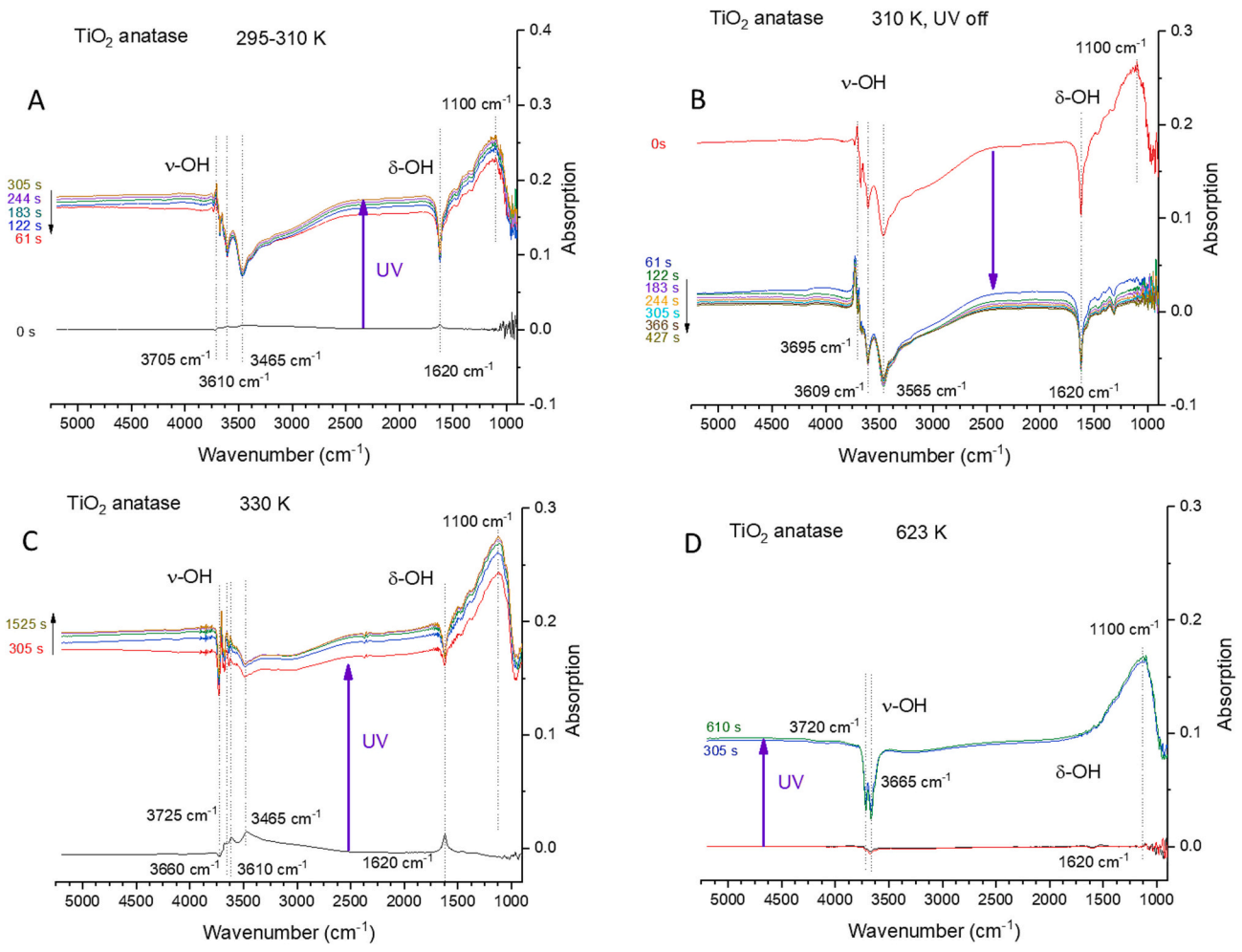

Fig. 1. DRIFT of TiO_2 anatase upon UV excitation (A, C, and D) under Ar flow at the indicated temperatures. UV flux = 2.7 W/cm^2. B. DRIFT of TiO_2 anatase once UV light is turned off at 310 K.

extra electron hops from one site to the other before they vanish by other reactions [26,27]. These polarons are classified by their size, small [28] and large [29]. TiO_2 rutile is known to have small polarons (equivalent to a unit cell or so) while TiO_2 anatase has large polarons (many unit cells) with a band-like structure and can extend to hundreds or thousands of unit cells; giving them a free-carrier- like coherent motion. They are traditionally seen by EPR [30], but can be studied by other techniques such as IR [31,32], pump probe time resolved spectroscopy [33] and core/valence level spectroscopy [34]. They show stability in vacuum or at low temperatures in some cases for hours [35].

This work is an attempt to probe into the role of these polarons as well conduction band electrons on the reaction selectivity during ethanol-TPD. From a chemical perspective we view both CB electrons and polarons to have similar effect since the activation energy needed for polaron migration is very small when compared to that required for a reaction to occur. To conduct the work, anatase powder was exposed to ethanol and UV light prior to TPD runs. Because ethanol traps holes formed under UV, conduction band electrons would therefore have a chance to accumulate and make the surface and near surface more metallic like. It is important to mention that this is different from making Ti^{3+} thermally. In thermal reaction, Ti^{3+} are formed because an oxygen atom has been removed from the lattice [36], while in a photoexcited system these Ti^{3+} cations are formed by electron transfer from the valence band without the removal of lattice oxygen.

2. Experimental

Temperature Programmed Desorption (TPD) studies were performed using 50 mg of TiO_2 placed in a quartz U-shaped fixed bed reactor connected to a vacuum system. The reactor was pumped with a scroll pump and had a base pressure of 1.5×10^{-3} Torr. TiO_2 (anatase) is supplied by Aldrich (637,254 100 mg; lot number MKBF78216V) in the form of nano-powder with a BET surface area of 45–55 m^2/g, with a size <25 nm and with a purity of 99.7 % (metal basis). The reactor was connected to a mass spectrometer chamber through a leak valve which had a typical base pressure $< 10^{-8}$ Torr maintained by a turbo molecular pump. A quadrupole mass spectrometer (Hiden) was used to monitor the masses of interest. Linear temperature ramping at 20 K min^{-1} was achieved by using an accurate temperature ramping unit, which consisted of a temperature controller (Eurotherm Process Control Unit and a 640 W power supply) integrated with a vertical tube furnace and a K type thermocouple. The thermocouple was inserted very close to the catalyst to measure the catalyst temperature. UV was supplied using a UV lamp (UVP UV-LS-25 EL series) installed at the top of the furnace containing the reactor. For each individual experiment, the catalyst was heated in vacuum at 673 K overnight. After that the catalyst was cooled to room temperature and pumped to its base pressure. A given amount of ethanol, 10, 50, or 100 μL was injected into the reactor through a rubber septum using a μL syringe. Still under ethanol environment, the catalyst was exposed to UV radiation to obtain a desired UV exposure. The reactor was then pumped down to its base pressure, then the UV light

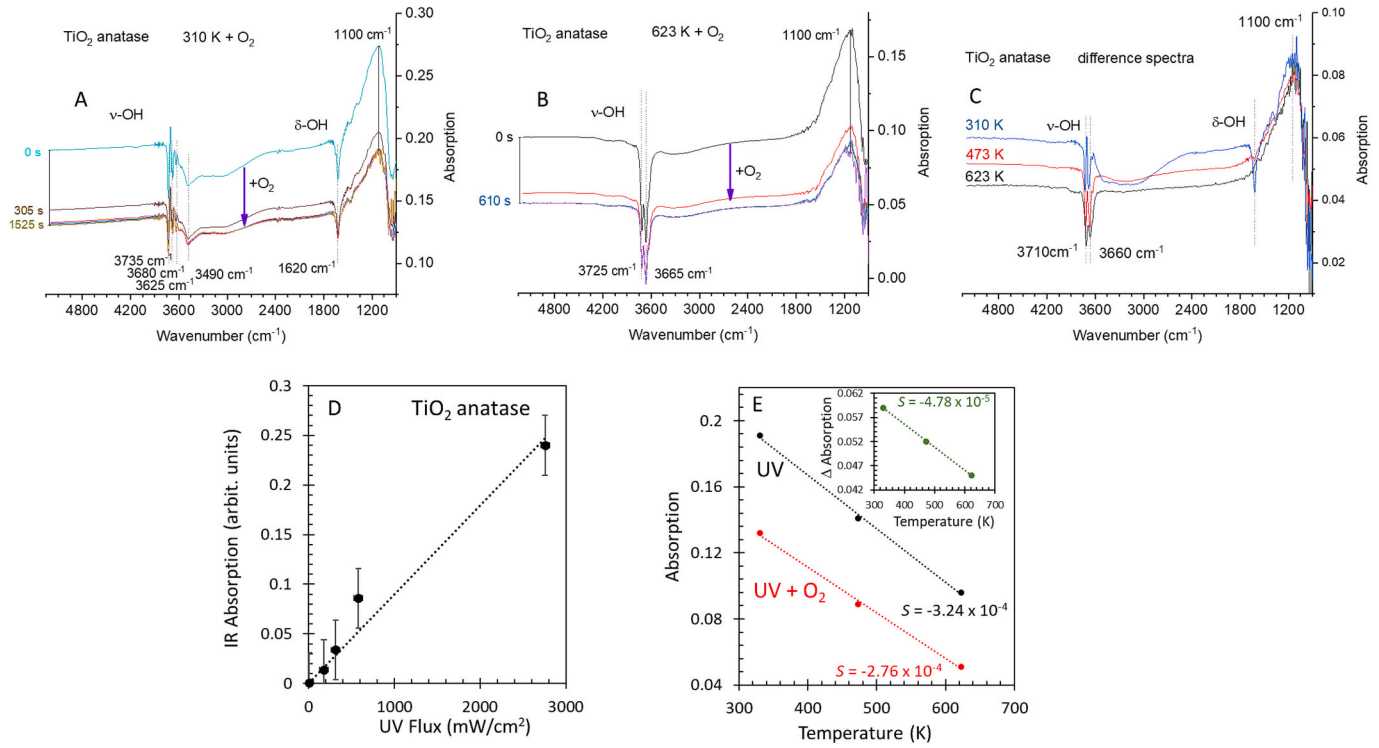

Fig. 2. Effect of O_2 on the IR signal from TiO_2 anatase in the presence of UV light (2.7 W/cm^2), A, B, C, and E). D. Effect of UV light flux on the IR signal of TiO_2 anatase (IR absorbance is taken in a flat region of the base line, 2000 cm^{-1}). A. 310 K. B. 623 K. C. difference spectra between UV and UV + O_2 at the indicated temperatures. E. Plot of the IR intensity signal at 4500 cm^{-1} in the presence of UV and UV + O_2 as a function of temperature; inset: the difference between the two straight lines in the main figure as a function of temperature.

being turned off before the start of the TPD experiments. The ethanol mass fragment $m/z = 31$ $(CH_2OH)^+$ was monitored until the measurement returned to baseline. Different mass fragments were recorded as a function of temperature to monitor the desorption of products, i.e. ethanol ($m/z = 31, 29, 45, 27$), acetaldehyde (m/z = 29, 44, 15, 43), ethylene (m/z = 28, 27), methane (m/z = 16,15) water (m/z = 18,17), H_2 (m/z = 2), CO (m/z = 28, 16), CO_2 (m/z = 44). A detailed account of TPD data analysis can be found elsewhere [37]. Acetaldehyde, ethylene, H_2O and H_2 were the main products that desorbed. The quantification of H_2 and H_2O were not included in this study due to contribution of signal from multiple sources that makes their quantification unreliable. The relative yields of all desorption products were determined by adopting the method described previously [38] while mass spectrometer sensitivity factor was calculated using the method described by Ko et al. [39]

IR experiments were conducted using a Bruker FTIR Vertex 80 machine equipped with a DRIFTS cell for sample treatment and measurements. TiO_2 anatase (alpha Aeasar, BET surface area = 45 m_2/g, Lot K26Y018) was placed inside the cell on top of the heating crucible. The powder was at about 45^o from the IR cell quartz window. The IR cell was heated with a Harrick ATK/Low voltage control unit. Gases were introduced using Bronkhorst EL-mass flow meters. A typical treatment was heating the powder in 20 % O_2 in Ar (99.999 %) at a flow of 40 mL/min from room temperatures to 700 K for a few hours then, switching to pure Ar before cooling under Ar flow. UV excitation was conducted using UV Fiber Spot Light source SAN-EI SUPERCURE - 204S, a 200 W Mercury Xenon lamp (Ozone free) from SAN-EI Electric Co., LTD, Osaka, Japan. Light fluencies were measured using Coherent Field Master GS power analyzer. The UV (250 to 400 nm) and visible (400 to 1100 nm) lights were measured using Coherent head sensors 12E61 (diameter, d = 6.0 mm) and 12,933 (d = 7.9 mm), respectively. For the UV light fluence measurements, the IR cell window was placed in between the source and the detector. The IR spectra are subtracted from that of the same crystal at the same temperature before UV-excitation.

3. Results

A. DRIFT – TiO_2 (anatase) with UV

Fig. 1 presents the effect of UV light on the IR signal at different temperatures of a fresh sample of polycrystalline anatase in the 900–5250 cm^{-1}; the signal below 900 cm^{-1} was too noisy to analyze. No IR cut off filter was used, and some heat was generated during excitation with UV, the temperature at the end of the experiment increased to about 310 K from 295 K in Fig. 1 A. While many works have been conducted on TiO_2 rutile and TiO_2 P25 (anatase/rutile) polycrystalline, we are aware of two studies on the effect of UV on TiO_2 anatase [40] by IR, one of them is in the liquid phase [41], prior to this work.

Upon UV excitation three changes in the spectrum occurred. (i) A rise in the absorption which is typical of TiO_2 in this region. This rise is due to conduction band electrons. The use of IR light provided the needed energy to displace trapped electrons in shallow sites (viewed as self-trapped electrons in the lattice, polarons) into the conduction band. The signal may also include intra band excitation. The response of the IR absorption signal to the light flux was tested (Fig. 2 D). Within experimental results there is a linear increase of the absorption with increasing light flux; deviation from linearity occurs at much higher fluxes [42] in the range of tens of MW/cm^2. (ii) The second observation is the negative signal related to removal of some adsorbed water and surface hydroxyls. This can be seen by the negative signal related to the bending mode of water (δ-H_2O) at ca. 1620 cm^{-1} and sharp signals in the 3400–3700 cm^{-1} related to the ν-OH of different types of surface hydroxyls. The negative broad band from about 3100 to 3700 cm^{-1} underneath the sharp negative signals is due to molecularly adsorbed water. (iii) The third observation is the appearance of a wide band centered at about 1100 cm^{-1}. The signal goes back down to its original absorption value once the UV is turned off (Fig. 1 B). The negative signals did not reverse indicting that surface depletion of these hydroxyls and adsorbed water

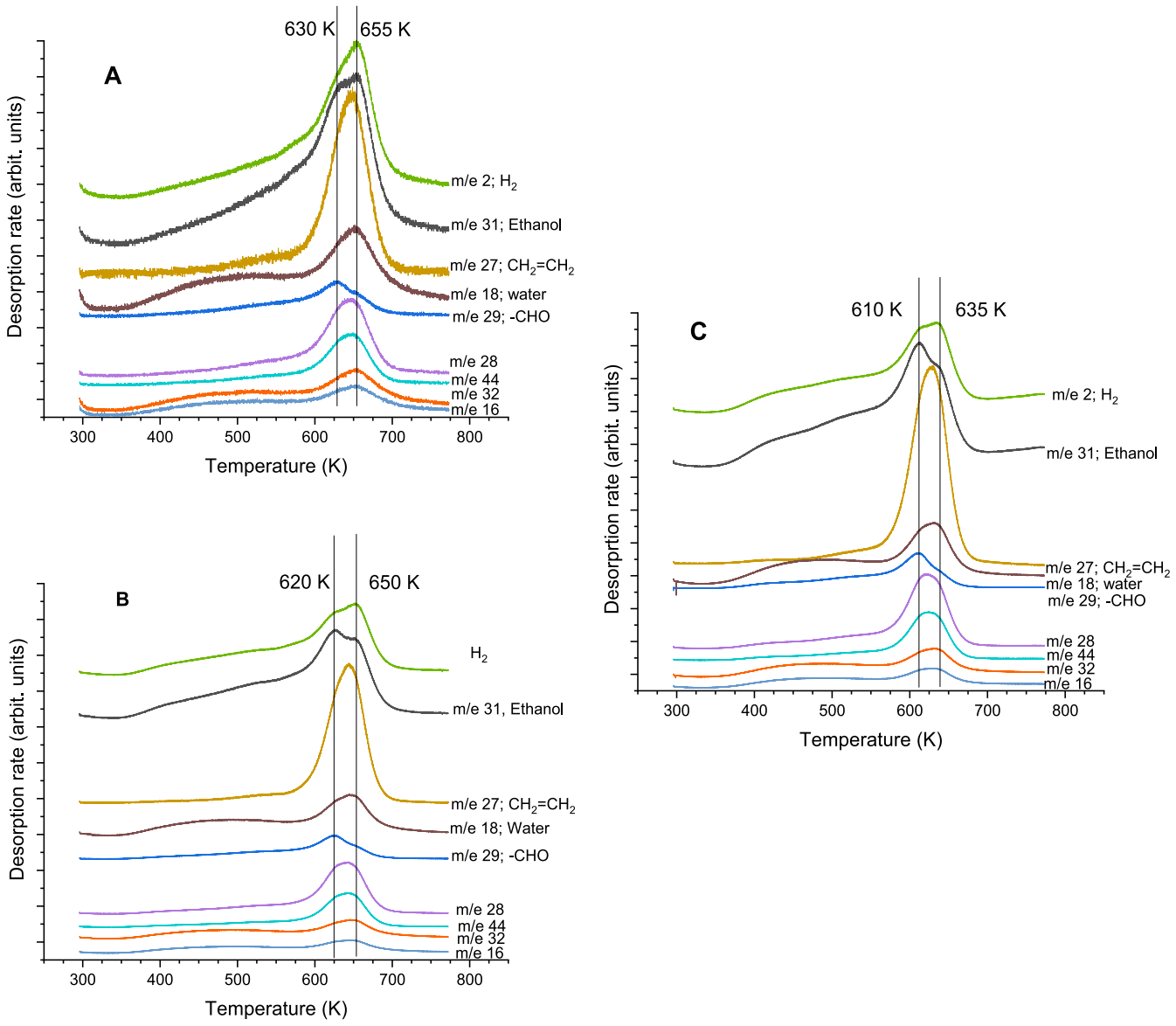

Fig. 3. As recorded products desorption during Ethanol-TPD over TiO_2 anatase (50 mg): at different initial exposure (A:10, B:50 and C:100 μL). These volumes equate to a ratio molecules of ethanol to surface atoms (Ti + O) ≈ 4, 20, and 40 respectively.

was irreversible at the given experimental conditions.

Increasing the temperature to 330 K, showed largely the same effect with and without UV, with the exception of the decrease of the molecularly adsorbed water contribution (Fig. 1 C). This trend is maintained up to the highest temperature investigated 623 K (Fig. 1 D) with the noticeable disappearance of water and most surface hydroxyls at high temperatures. Another observation is related to the magnitude of the absolute IR signal upon UV excitation, increasing the temperature resulted in decreasing the IR signal rise. This is due to the negative effect of temperature on conduction band electrons because with increasing temperature the electron -hole recombination rate is poised to increase and therefore, the population density of conduction band electrons decreases. There is, however, no change in the shape of the peak centered at 1100 cm^{-1} with temperature.

Fig. 2 (A and B) presents the effect of O_2 on the signal of these conduction band electrons at 330 and 623 K. O_2 reacts with conduction band electrons to give O_2^- (O_2 minus radical) and therefore decreases their population. This has been seen before by EPR [43,44], pump probe time resolved spectroscopy [45], as well as by photoluminescence [46,47] on n-type semiconductors. The decrease due to quenching of these conduction band electrons is constant with time under O_2.

It is not clear if the magnitude of the decrease is equally sensitive to temperature from 900 to 5250 cm^{-1} or not because there is a non-linear effect on the absorption in each spectrum. A subtraction of the IR signal under O_2 plus UV light from that under Ar plus UV light is shown in Fig. 2 C. The subtraction is conducted for the raw spectra without normalization nor offset. As seen in Fig. 2 C, within reproducibility the peak centered at about 1100 cm^{-1} is largely the same at the three investigated temperatures (330, 473, and 623 K) yet the base line at the high frequency range is not the same. While O_2 reacts with the surface of TiO_2, the IR signal originates from surface and bulk conduction band electrons. In other words, the decrease of the IR signal in the presence of O_2 is due to consumption of excited surface excess electrons as well those diffused from the bulk. Some sections in this frequency range might be more sensitive to surface population then others causing such a change. Fig. 2 E shows a plot of the IR signal at these three temperatures under UV as well as under UV + O_2. The slight change in the slope between two lines indicates that that CB electrons consumption by O_2 may also be a function of temperature (assuming that $P_{O2} >>$ larger than the number of surface sites). The inset shows the difference between the two

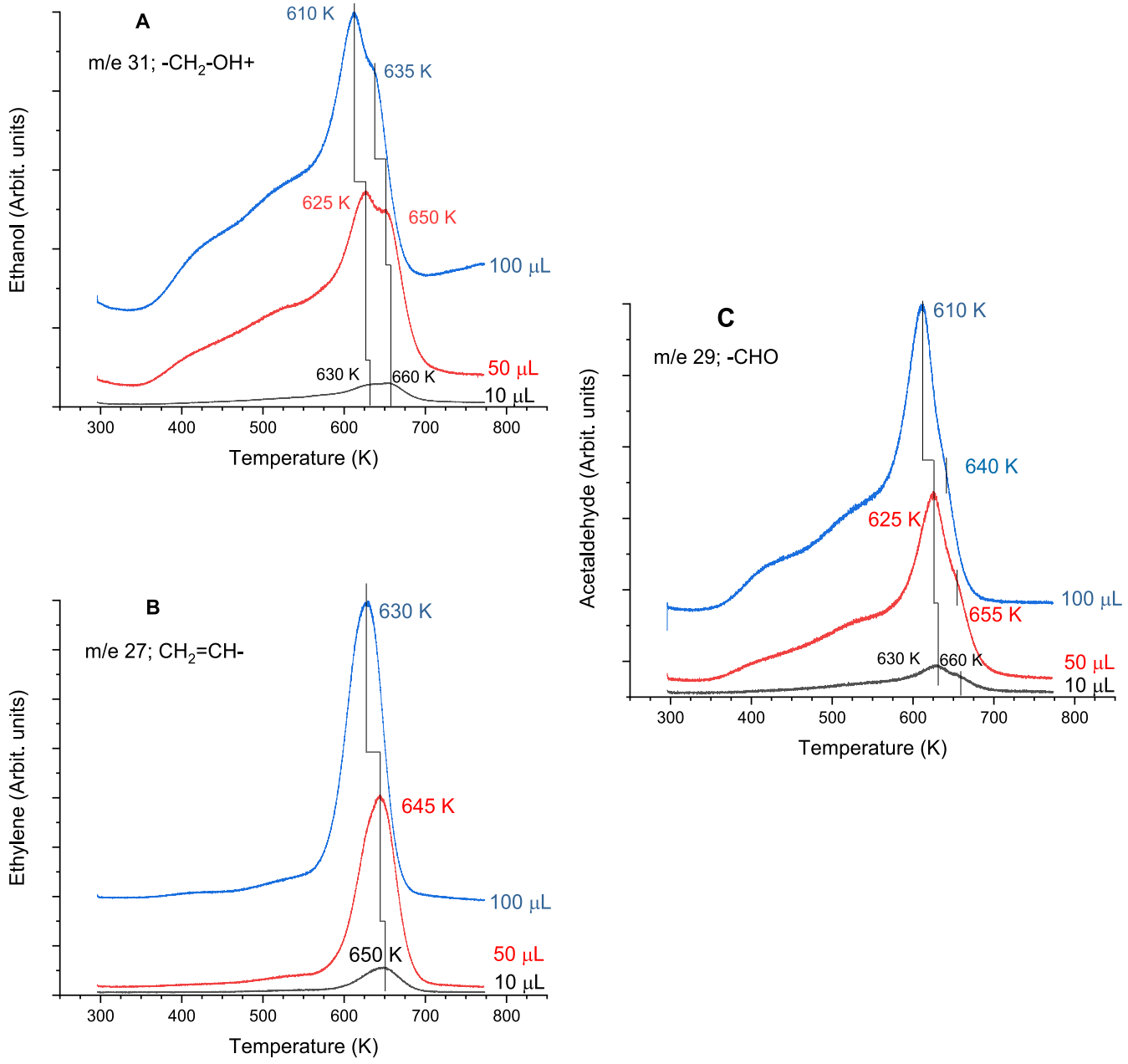

Fig. 4. Ethanol-TPD over TiO_2 anatase (50 mg): at different initial exposure. 10, 50 and 100 µL equate to a ratio molecules of ethanol to surface atoms (Ti + O) ≈ 4, 20, and 40 respectively. A: Ethanol desorption; B: Ethylene desorption; C: acetaldehyde desorption. Ethanol contribution in m/e 27 (m/e 31 signal × 0.23) and m/e 29 (m/e 31 signal × 0.28) for ethylene and acetaldehyde, respectively, are subtracted in the desorption profiles.

lines taken at 4500 cm^{-1} as a function of temperature in which a decrease with increase in temperature is noticed. An estimate of the activation energy of the effect of temperature on the IR signal of these CB electrons can be obtained from an Arrhenius plot (Ln (I_{abs}) vs $1/T$, where I_{abs} is the IR absorption and T is temperature in K). An activation energy of about 40 meV is extracted in the absence of O_2 and 55 meV in its presence.

B. Ethanol TPD over TiO_2 anatase.

B.1 TiO2 anatase not exposed to UV light prior to TPD

Fig. 3 (A, B and C) presents ethanol-TPD after three different exposures on anatase TiO_2. The desorption profile is very similar in the three cases. From 300 to ca. 550 K there is a broad week desorption of most masses with water and ethanol having the largest contribution. The main desorption of reaction products and unreacted ethanol is seen in the 600 to 750 K region. In this temperature domain there are two desorption channels separated by about 30 K. At low exposure (Fig. 3 A) the high temperature channel at 655 K is the most pronounced. Reaction products are ethylene (m/e 27), acetaldehyde (m/e 29), methane (m/e 16 and 15), in addition to CO, CO_2 and H_2. Fragmentation patterns subtraction to differentiate between the reaction products is given in the experimental section. Some qualitative differences can also be seen and are used to further identify the reaction products. For example, m/e 44 has a contribution from acetaldehyde and CO_2. Acetaldehyde with a MW 44, but parent mass m/e 29 desorbs in two temperatures at 630 and 655 K with the first being more pronounced than the second while CO_2 desorb as a wide peak covering both temperatures. Increasing exposure results in increasing the signal of the first temperature when compared to the second for all products (see Fig. 4 in the case of ethanol,

Table 1
Peak areas of the main fragmentations desorbing during ethanol TPD on TiO_2 anatase at different exposures. a: ratio acetaldehyde (m/e 29) to ethylene (m/e 27).

	10 μL			50 μL			100 μL		
Mass spectrometer fragment	Peak area (arbit. Units)	Relative yield to ethanol	ratio[a]	Peak area (arbit. Units)	Relative yield to ethanol	ratio[a]	Peak area (arbit. Units)	Relative yield to ethanol	ratio[a]
m/e 2 (H_2)	$8.2\ 10^{-8}$	0.82		$4.9\ 10^{-7}$	0.75		–	–	
m/e 31 (ethanol)	$1.0\ 10^{-7}$	1.00		$6.5\ 10^{-7}$	1.00		$8.5\ 10^{-7}$	1.00	
m/e 27	$7.0\ 10^{-8}$	0.70		$4.9\ 10^{-7}$	0.75		$7.4\ 10^{-7}$	0.87	
m/e 18 (water)	$5.4\ 10^{-8}$	0.54		$2.8\ 10^{-7}$	0.43		$3.9\ 10^{-7}$	0.46	
m/e 29	$1.9\ 10^{-8}$	0.19	0.27	$1.4\ 10^{-7}$	0.22	0.28	$2.1\ 10^{-7}$	0.25	0.28
m/e 28	$3.7\ 10^{-8}$	0.37		$2.5\ 10^{-7}$	0.38		$3.6\ 10^{-7}$	0.42	
m/e 44	$2.4\ 10^{-8}$	0.24		$1.6\ 10^{-7}$	0.25		$2.3\ 10^{-7}$	0.27	
m/e 16	$2.1\ 10^{-8}$	0.21		$1.1\ 10^{-7}$	0.17		$1.4\ 10^{-7}$	0.16	

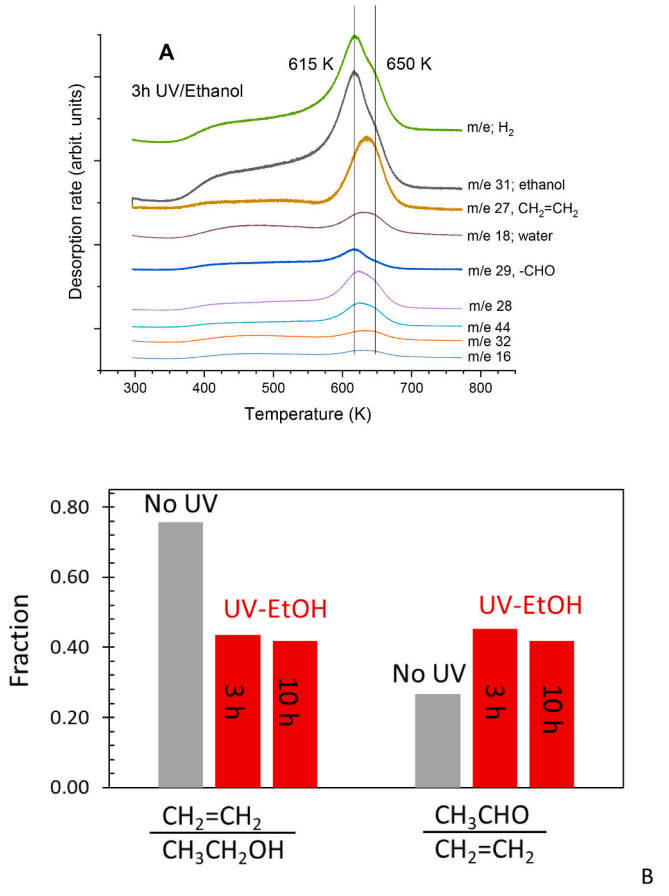

Fig. 5. As recorded products desorption during Ethanol-TPD over TiO_2 anatase (50 mg) that was prior exposed to UV light in the presence of ethanol for 3 h (A). Ethanol exposure prior to TPD is 50 μL which corresponds to ratio molecules of ethanol to surface atoms (Ti + O) ≈ 20. B. The first three columns represent the fraction of ethylene over the reactant ethanol and the next three columns are for the fraction of acetaldehyde to ethylene (the main reaction products) during Ethanol TPD over TiO_2 anatase. Grey columns are for ethanol-TPD on non-irradiated TiO_2 while red columns are for ethanol-TPD after TiO_2 that was prior irradiated with UV in the presence of 50 μL of ethanol at the given time. (For interpretation of the references to colour in this figure legend, the reader is referred to the web version of this article.)

acetaldehyde, and ethylene). Both temperatures shift to lower values with increasing exposure which is most plausibly attributed to lateral repulsive interactions between adsorbed ethanol in its molecular and or dissociated mode. The origin of the two desorption temperatures at 610–630 and 635-655 K is not known. However, the low temperature desorption is associated with the dehydrogenation to acetaldehyde while the second is associated with the dehydration to ethylene in addition to total decomposition. The fact that both peaks shift by about the same values with increasing exposure may indicate that they originate from two types of surface sites. The dominant surface orientation of anatase is the (101) and other orientations may also be present such as the (100) and (001). If for example the high temperature desorption is due to oxygen defects one would have expected it to saturate and do not shift. Therefore, such as pathway may be neglected. STM results of TiO_2(101) anatase show that oxygen defects are subsurface [9], which would have less or no effect on the modes of adsorption of ethanol. Computation studies of ethanol (as well as methanol) on anatase show that both molecular and dissociative modes have very close adsorption energies and this further complicates the assignment [9]. Further analyses are given below (section B.2) when we compare ethanol-TPD on TiO_2 that was prior exposed to UV light from which more insights may be gained.

Table 1 shows the relative computed areas (with respect to ethanol) for all peaks as desorbed during TPD. While some quantitative differences occur, it seems that changes in the coverage does not cause dramatic changes in reaction selectivity. For example, while the relative yield of m/e 29 (acetaldehyde) and m/e 27 (ethylene) slightly increased with exposure, their ratio was the same.

B.2 TPD of ethanol after exposing TiO_2 anatase to UV + ethanol to stabilize conduction band electrons

Ethanol-TPD was then conducted over TiO_2 anatase that was exposed to ethanol + UV for prolonged time (3 h and 10 h), the long periods were preferred because of the weak UV flux of the lamp used (0.08 W/cm^2) in this part of the study. TPD of the prior three hours irradiated TiO_2 anatase in the presence of ethanol (50 μL) is shown in Fig. 5 A (the one after ten hours gave very similar results). All peaks observed on non-irradiated TiO_2 are present too. However, two main differences can be seen and most likely related to each other. Ethylene yield decreased compared to acetaldehyde (Fig. 5 B) and a different shape for hydrogen desorption occurred. Below, a plausible explanation is given.

Exposing a UV irradiated TiO_2 to ethanol results in accumulation of electrons in the conduction band, because ethanol traps holes decreasing the e-h recombination rate.

$$TiO_2 + UV \rightarrow e + h \quad (1)$$

$$CH_3CH_2OH_{(a)} + h \rightarrow CH_3CHO + 2\,[H] + e \quad (2)$$

(a): adsorbed

Actually, an ethanol molecule (or more accurately an ethoxide species) injects one electron into the CB (to trap a hole) and a second electron into the CB (current doubling effect) [48]. In the presence of a noble metal the 2 [H] (which is in the form of a proton of a surface hydroxyl, -OH) react with these two electrons to generate H_2. In the absence of a metal, as in this case, H_2 is not produced (or with neglible amount when compared to that in the presence of a metal, 10–50 times less) [49] and electrons are accumulated in the CB for a period of time; see for example Fig. 3 in ref. 34. This makes TiO_2 more metallic which in turn decreases the dehydration to ethylene pathway. This is because metals decompose or dehydrogenate primary alcohols and we are not

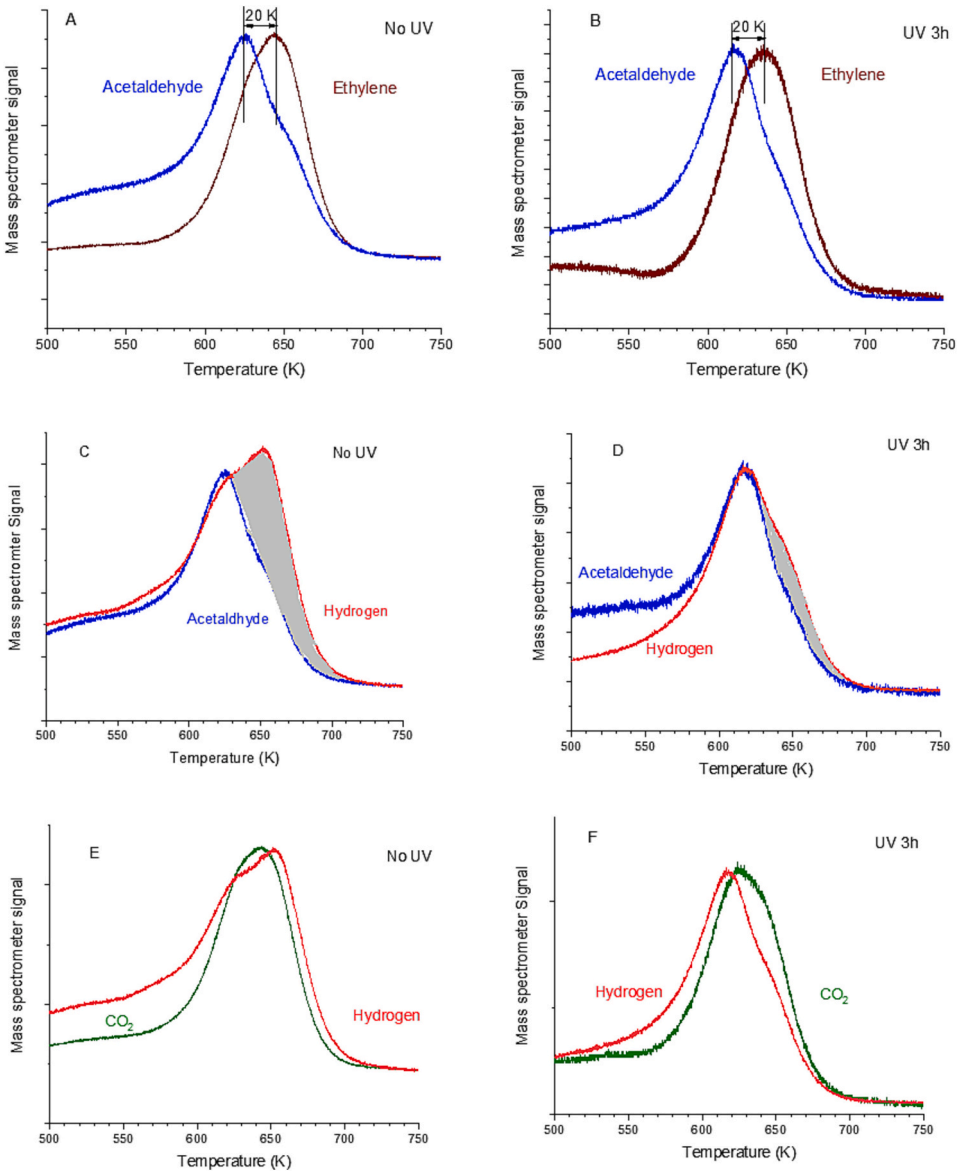

Fig. 6. Selected products desorbing during ethanol-TPD over anatase TiO_2. A, C, E in the absence of UV. B, D, F after UV excitation for 3 h. The high temperature channel is attributed to products of total decomposition (oxidation) that is partly suppressed on the prior UV excited sample.

aware of dehydration reactions of primary alcohols on metals. Moreover, this will affect the decomposition pathway. In the absence of UV light, the decomposition of ethanol gives the following products.

$$CH_3CH_2OH_{(a)} + [O]_{surface} \rightarrow CO_2 + H_2 + CH_4 \quad (3)$$

On the surface of TiO_2 with excess electrons this pathway appears to be partly suppressed increasing, thus, the yield of acetaldehyde.

$$CH_3CH_2OH_{(a)} \rightarrow CH_3CHO_{(g)} + H_2 \quad (4)$$

(g): gas

We do not know the population density of these excess electrons in the conduction band prior to the reaction nor at the reaction temperature (600–650 K). These most likely change with treatments. Because the activation energy for the disappearance of these polarons as extracted from Fig. 2 is very small (40 meV in the absence of O_2 or 55 meV in its presence) the fraction of these charges (Ti^{3+}) at 650 K would be still very high (ca. 0.8). Eq. 3 (pathway 1) occurs at ca. 650 K while eq. 4 (pathway 2) is at about 610 K. This is better illustrated in Fig. 6 in which acetaldehyde and ethylene (Fig. 6 A, B), H_2 and acetaldehyde (Fig. 6 C, D) and H_2 and CO_2 (Fig. 6 E, F) desorptions are overlaid. To do this, spectra are aligned to better highlight the difference. In all cases studied, coverage effect or UV light effect, ethylene desorbs at a higher temperature than acetaldehyde (in this work by about 20 K). This seems to be a more general observation. Recent work of ethanol TPD on UO_2 thin film also showed that ethylene desorbs about 20 K higher than acetaldehyde [50]. The high temperature in which ethylene desorbs also has contribution from CO_2 and H_2 desorption. Yet H_2 desorption is different on the post irradiated TiO_2. In this case it tracked acetaldehyde and not CO_2 (Fig. 6). This might be linked to the presence of excess electrons partly suppressing the oxidation pathway (eq. 3). It is important to mention that while excess electrons might be the reasons, these are not associated to surface oxygen defects, since UV excitation does not create surface oxygen vacancies. The effect might be a screening of the oxidation process due to change in metallicity of the surface and near surface, favoring the channel for dehydrogenation (eq. 4).

4. Conclusions

UV Photo-irradiation of TiO_2 anatase was studied by IR in order to track the changes in conduction band electrons with temperature

(300–623 K) and with gas phase O_2. The rise in the IR base line upon UV excitation (due to conduction band electrons originated from excited large polarons) decreased with increasing temperature (attributed to an accelerated e-h recombination rate) and in the presence of O_2 (attributed to trapping of CB electrons). The associated activation energies of the signal rise upon excitation were 40 and 55 meV in the absence and in the presence of O_2. These CB electrons resulting from self-trapped large polarons in TiO_2 anatase give it a metallic like property. To probe the effect of these polarons on chemical reactions TPD of ethanol was studied. Over the non-prior irradiated TiO_2 anatase, the main reaction products, acetaldehyde and ethylene, desorbed at 630 and 650 K, respectively, with ethylene (the dehydration product) being the dominant one. Over TiO_2 that was prior UV-irradiated in the presence of ethanol (to trap holes and increase the population of CB electrons) the pathway to the dehydrogenation product acetaldehyde was more pronounced and in addition the oxidation products were largely suppressed. We attribute these changes to the increased metallicity of TiO_2 anatase because of the increased population of CB electrons.

Supplementary data to this article can be found online at https://doi.org/10.1016/j.cplett.2025.141965.

CRediT authorship contribution statement

M.A. Nadeem: Methodology, Investigation, Formal analysis, Data curation. **H. Idriss:** Writing – review & editing, Writing – original draft, Methodology, Investigation, Formal analysis, Conceptualization.

Declaration of competing interest

The authors declare that they have no known competing financial interests or personal relationships that could have appeared to influence the work reported in this paper.

Acknowledgment

HI thanks Stefan Heissler (IFG) for providing the UV lamp and detectors for light calibration.

Data availability

Data will be made available on request.

References

[1] D. Vazquez-Pargá, A. Jurado, A. Roldan, F. Vines, A computational map of the probe CO molecule adsorption and dissociation on transition metal low miller indices surfaces, Appl. Surf. Sci. 618 (2023) 156581.
[2] H. Shulz, Short history and present trends of Fischer–Tropsch synthesis, Appl. Catal. A: General 186 (1999) 3–12.
[3] J.C. Védrine, Heterogeneous partial (amm)oxidation and oxidative dehydrogenation catalysis on mixed metal oxides, Catalysts 2 (2016) 1–26.
[4] J.H. Carter, T. Bere, J.R. Pitchers, D.G. Hewes, B.D. Vandegehuchte, C.J. Kiely, S. H. Taylor, G.J. Hutchings, Direct and oxidative dehydrogenation of propane: from catalyst design to industrial application, Green Chem. 23 (2021) 9747–9799.
[5] J.M. Vohs, M.A. Barteau, Dehydration and dehydrogenation of ethanol and i-propanol on the polar surfaces of zinc oxide, Surf. Sci. 221 (1989) 590–608.
[6] P. Kostestkyy, J. Yu, R.J. Gorte, G. Mpourmpakis, T. Zaki, Structure–activity relationships on metal-oxides: alcohol dehydration, Catal, Sci. Technol. 4 (2014) 3861–3869.
[7] S. Afrin, P. Bollini, A transient kinetic analysis of the evolution of a reducible metal oxide towards catalyzing nonoxidative alkanol dehydrogenation, J. Catal. 393 (2021) 290–302.
[8] K. Katsiev, G. Harrison, H. Alghamdi, Y. Alsalik, A. Wilson, G. Thornton, H. Idriss, Mechanism of ethanol photooxidation on single-crystal anatase TiO_2(101), J. Phys. Chem. C 121 (2017) 2940–2950.
[9] R. Zhang, Z. Liu, L. Ling, B. Wang, The effect of anatase TiO_2 surface structure on the behavior of ethanol adsorption and its initial dissociation step: a DFT study, Appl. Surf. Sci. 353 (2015) 150–157.
[10] A.M. Nadeem, G.I.N. Waterhouse, H. Idriss, The reactions of ethanol on TiO_2 and au/TiO_2 anatase catalysts, Catal. Today 182 (2012) 16–24.
[11] E. Farfan-Arribas, R.J. Madix, Role of defects in the adsorption of aliphatic alcohols on the TiO_2(110) surface, J. Phys. Chem. B 106 (2002) 10680–10692.
[12] H. Idriss, K.S. Kim, M.A. Barteau, Carbon-carbon bond formation via aldolization of acetaldehyde on single crystal and polycrystalline TiO_2 surfaces, J. Catal. 139 (1993) 119–133.
[13] V.V. Kaichev, Y.A. Chesalov, A.A. Saraev, A.Y. Klyushin, A. Knop-Gericke, T. V. Andrushkevich, V.I. Bukhtiyarov, Redox mechanism for selective oxidation of ethanol over monolayer V_2O_5/TiO_2 catalysts, J. Catal. 338 (2016) 82–93.
[14] S. Melchers, J. Schneider, A.V. Emeline, D.W. Bahnemann, Effect of H_2O and O_2 on the adsorption and degradation of acetaldehyde on anatase surfaces—an in-situ ATR-FTIR study, Catalysts 8 (417) (2018) 1–12.
[15] H. Idriss, M. Scott, J. Llorca, S.C. Chan, W. Chiu, P.Y. Sheng, A. Yee, M. A. Blackford, S.J. Pas, A.J. Hill, F.M. Alamgir, R. Rettew, C. Petersburg, S. Senanayake, M.A. Barteau, A phenomenological study of the metal/oxide interface. The role of catalysis in hydrogen production from renewable sources, Chem. Sus. Chem. 1 (2008) 905–910.
[16] I.R. Bellobono, F. Morazzoni, R. Bianchi, E.S. Mangone, R. Stanescu, C. Costache, P. M. Tozzi, Laboratory-scale photomineralisation of n-alkanes in aqueous solution, by photocatalytic membranes immobilising titanium dioxide, Int. J. Photoenergy 7 (2005) 79–85.
[17] G.P. Lepore, A. Vlček Jr., C.H. Langford, in: D.F. Ollis, H. Al-Ekabi (Eds.), Photo-Catalytic Purification and Treatment of Water and Air, Elsevier, Amster-dam, NL, 1993.
[18] Z.H.N. Al-Azri, W.T. Chen, A. Chan, V. Jovic, T. Ina, H. Idriss, G.I.N. Waterhouse, The roles of metal co-catalysts and reaction media in photocatalytic hydrogen production: performance evaluation of M/TiO_2 photocatalysts (M= Pd, Pt, au) in different alcohol-water mixtures, J. Catal. 329 (2015) 355–367.
[19] M. Bowker, W.J. Phil, Methanol photo-reforming with water on pure titania for hydrogen production, Trans. R. Soc. A 378 (2020) 20200058.
[20] K. Katsiev, G. Harrison, Y. Al-Salik, G. Thornton, H. Idriss, Gold cluster coverage effect on H_2 production over rutile TiO_2(110), ACS Catal. 9 (2019) 8294–8305.
[21] J.B. Joo, R. Dillon, I. Lee, Y. Yin, C.J. Bardeen, F. Zaera, Promotion of atomic hydrogen recombination as an alternative to electron trapping for the role of metals in the photocatalytic production of H_2, Proc. Natl. Acad. Sci. 111 (2014) 7942–7947.
[22] M.A. Nadeem, H. Idriss, Photo-thermal enhancement of ethanol reactions on ag supported on TiO_2 catalyst, Chem. Comm. 54 (2018) 5197–5200.
[23] M.A. Nadeem, H. Idriss, Effect of temperature on photoreactions of ethanol on ag/TiO_2 catalyst under steady state conditions, Appl. Catal. B Env. 284 (119736) (2021) 1–9.
[24] C.D. Valentin, D. Fittipaldi, Hole scavenging by organic adsorbates on the TiO_2 surface: a DFT model study, J. Phys. Chem. Lett. 4 (2013) 1901–1906.
[25] H. Alghamdi, H. Idriss, Study of the modes of adsorption and electronic structure of hydrogen peroxide and ethanol over TiO_2 rutile (110) surface within the context of water splitting, Surf. Sci. 669 (2018) 103–113.
[26] I.G. Austin, N.F. Mott, Polarons in crystalline and non-crystalline materials, Adv. Phys. 50 (2001) 757–812.
[27] M. Reticcioli, M. Setvin, M. Schmid, U. Diebold, C. Franchini, Formation and dynamics of small polarons on the rutile TiO_2(110) surface, Phys. Rev. B 8 (2018) 045306.
[28] J. Chen, C. Penschke, A. Alavi, A. Michaelides, Small polarons and the Janus nature of TiO_2 (110), Phys. Rev. B 101 (2020) 115402.
[29] S. Moser, L. Moreschini, J. Jaćimović, O.S. Barišić, H. Berger, A. Magrez, Y. J. Chang, K.S. Kim, A. Bostwick, E. Rotenberg, J. Forró, M. Grioni, Tunable polaronic conduction in anatase TiO_2, Phys. Rev. Lett. 110 (2013) 196403.
[30] C.P. Kumar, N.O. Gopal, T.C. Wang, M.-S. Wong, S.C. Ke, EPR investigation of TiO_2 nanoparticles with temperature-dependent properties, J. Phys. Chem. B 110 (2006) 5223–5229.
[31] T. Berger, M. Sterrer, O. Diwald, E. Knozinger, D. Panayotov, T.L. Thompson, J. T. Yates Jr., Light-induced charge separation in anatase TiO_2 particles, J. Phys. Chem. B 109 (2005) 6061–6068.
[32] D.A. Panayotov, S.P. Burrows, J.R. Morris, Infrared spectroscopic studies of conduction band and trapped electrons in UV-photoexcited, H-atom n-doped, and thermally reduced TiO_2, J. Phys. Chem. C 116 (2012) 4535–4544.
[33] P. Maity, K. Katsiev, O.F. Mohammed, H. Idriss, Study of the bulk charge carrier dynamics in anatase and rutile TiO_2 single crystals by femtosecond time-resolved spectroscopy, J. Phys. Chem. C 122 (2018) 8925.
[34] Y. Al-Salik, K. Katsiev, H. Idriss, Electron transfer from excited semiconductor to metal particles and its implication on photocatalysis. The case of au/TiO_2(110) single crystal, J. Phys. Chem. C 126 (2022) 15184–15190.
[35] D.C. Hurum, A.G. Agrios, K.A. Gray, Explaining the enhanced photocatalytic activity of degussa P25 mixed-phase TiO_2 using EPR, J. Phys. Chem. B 107 (2003) 4545–4549.
[36] H. Idriss, Oxygen vacancies role in thermally driven and photon driven catalytic reactions, Chem. Catal. 2 (2022) 1549–1560.
[37] M.A. Nadeem, G.I.N. Waterhouse, H. Idriss, Study of ethanol reactions on H_2 reduced au/TiO_2 anatase and rutile: effect of metal loading on reaction selectivity, Catal. Struct. React. 1 (2015) 61–70.
[38] M.A. Nadeem, G.I.N. Waterhouse, H. Idriss, A study of ethanol reactions on O_2-treated au/TiO_2. Effect of support and metal loading on reaction selectivity, Surf. Sci. 650 (2016) 40–50.
[39] E.I. Ko, J.B. Benziger, R.J. Madix, Reactions of methanol on W(100) and W(100)-(5 × 1)C surfaces, J. Catal. 62 (1980) 264–274.
[40] Z. Fu, H. Onishi, Infrared and near-infrared spectrometry of anatase and rutile particles bandgap excited in liquid, J. Phys. Chem. B 127 (2023) 321–327.
[41] D.M. Savory, A.J. McQuillan, IR spectroscopic behavior of polaronic trapped electrons in TiO_2 under aqueous photocatalytic conditions, J. Phys. Chem. C 118 (2014) 13680–13692.

[42] P. Herth, D. Schaniel, Th. Woike, T. Granzow, M. Imlau, E. Krätzig, Polarons generated by laser pulses in doped $LiNbO_3$, Phys. Rev. B 71 (2005), 125128 (1-10).
[43] J.M. Coronado, A.J. Maira, J.C. Conesa, K.L. Yeung, V. Augugliaro, J. Soria, EPR study of the surface characteristics of nanostructured TiO_2 under UV irradiation, Langmuir 17 (2001) 5368–5374.
[44] T. Berger, M. Sterrer, O. Diwald, E. Knozinger, Charge trapping and photoadsorption of O_2 on dehydroxylated TiO_2 nanocrystals—an electron paramagnetic resonance study, Chem. Phys. Chem. 6 (2005) 2104–2112.
[45] A. Yamakata, J.J.M. Vequizo, H. Matsunaga, Distinctive behavior of photogenerated electrons and holes in anatase and rutile TiO_2 powders, J. Phys. Chem. C 119 (2015) 24538–24545.
[46] H. Idriss, A. Barteau, Photoluminescence from zinc oxide powder to probe adsorption and reaction of oxygen, carbon monoxide, hydrogen, formic acid, and methanol, J. Phys. Chem. 96 (1992) 3382–3388.
[47] D.K. Pallotti, L. Passoni, P. Maddalena, F.D. Fonzo, S. Lettieri, Photoluminescence mechanisms in anatase and rutile TiO_2, J. Phys. Chem. C 121 (2017) 9011–9021.
[48] H. JonasØ, R. Bebensee, U. Martinez, S. Porsgaard, E. Lira, Y. Wei, L. Lammich, Z. Li, H. Idriss, F. Besenbacher, B. Hammer, S. Wendt, Unravelling site-specific photo-reactions of ethanol on rutile TiO_2(110), Sci. Rep. 6 (2016) 21990.
[49] E. Hussain, I. Majeed, M.A. Nadeem, A. Iqbal, Y. Chen, M. Choucair, R. Jin, M. A. Nadeem, Remarkable effect of BaO on photocatalytic H_2 evolution from water splitting via TiO_2 (P25) supported palladium nanoparticles, J. Env. Chem. Eng. 7 (2019) 102729.
[50] H. Idriss, T. Gouder, Surface reactions of ethanol on UO_2 thin film. Dehydrogenation and dehydration pathways, Appl. Surf. Sci. 683 (2025) 161716.